약학석사학위논문

Long circulating Ferritin Nanocage with 'Protein cloud'

혈중 반감기 향상을 위한 나노케이지 개발

2016년 8월

서울대학교 대학원

약학과 물리약학전공

이 나 경

Long circulating Ferritin Nanocage with 'Protein cloud'

혈중 반감기 향상을 위한 나노케이지 개발

지도교수 변 영 로

이 논문을 약학석사 학위논문으로 제출함

2016년 8월

서울대학교 대학원

약학과 물리약학 전공

이 나 경

이나경의 석사학위논문을 인준함

2016년 8월

위 원 장 오위경 (인)

부 위 원 장 김민산 (인)

위 원 변영로 (인)

Abstract

Protein nanocages have a wide range of applicability in research due to their favourable features, such as high biocompatibility, low toxicity profiles and capacity for genetic and chemical modification. Such an example are ferritin nanocages, endogenous in nature, that have been modified for use as delivery vehicles of therapeutic drugs and peptides in research. Here we have developed ferritin nanocages with an extended pharmacokinetic profile that can be used as a platform for application in research.

Protein-based agents are prone to rapid degradation *in vivo* and approaches such as PEGylation that can overcome this issue are continuously being pursued. Due to the heterogeneous nature of PEG itself, chemical conjugation of PEG leads to poor quality control of its products. However, fusion of XTEN, a peptide composed of hydrophilic amino acids, can be done in a one step recombinant protein synthesis with high yields using bacteria *E. coli*. Using previously developed XTEN peptides, a protein corona covering the outer surface of the nanocage was formed. Ferritin nanocages with the protein corona were synthesized through bacterial expression of the hybrid gene consisting of human ferritin heavy chain (hFTH), linker (glycine-rich peptide) and XTEN genes. The self-assembly of of hfTH leads to the formation of nanocages (12 nm in diameter), and varying lengths of XTEN peptides attached at the C-termini constitutes an outer layer of protein corona, resulting in the construction of FTH-XTEN nanocages.

These modified ferritin nanocages show lengthened half-lives *in vivo* and overall improved pharmacokinetic profiles as compared to ferritin alone. The half-lives of nanocages increase in correlation to increasing length of XTEN peptide attached. *In vitro* and *in vivo* characterizations of the developed FTH-XTEN nanocages are reported here, and these nanocages show potential for various applications in delivery of drugs and therapeutic peptides.

Key words: Protein-based nanocage, ferritin nanoparticle, XTEN, long-circulating

Master's in Pharmacy

Student number: 2014-22978

Thesis advisor: Professor Young-ro Byun

Table of contents

List of tables

List of figures

injection of FTH and FTH-XTEN nanocages labelled with Cy5-NHS Ester dye. Results show lengthened half-life, reduced volume of distribution as well as reduced rate of clearance with increasing length of XTEN peptide attached.

Schematic diagram

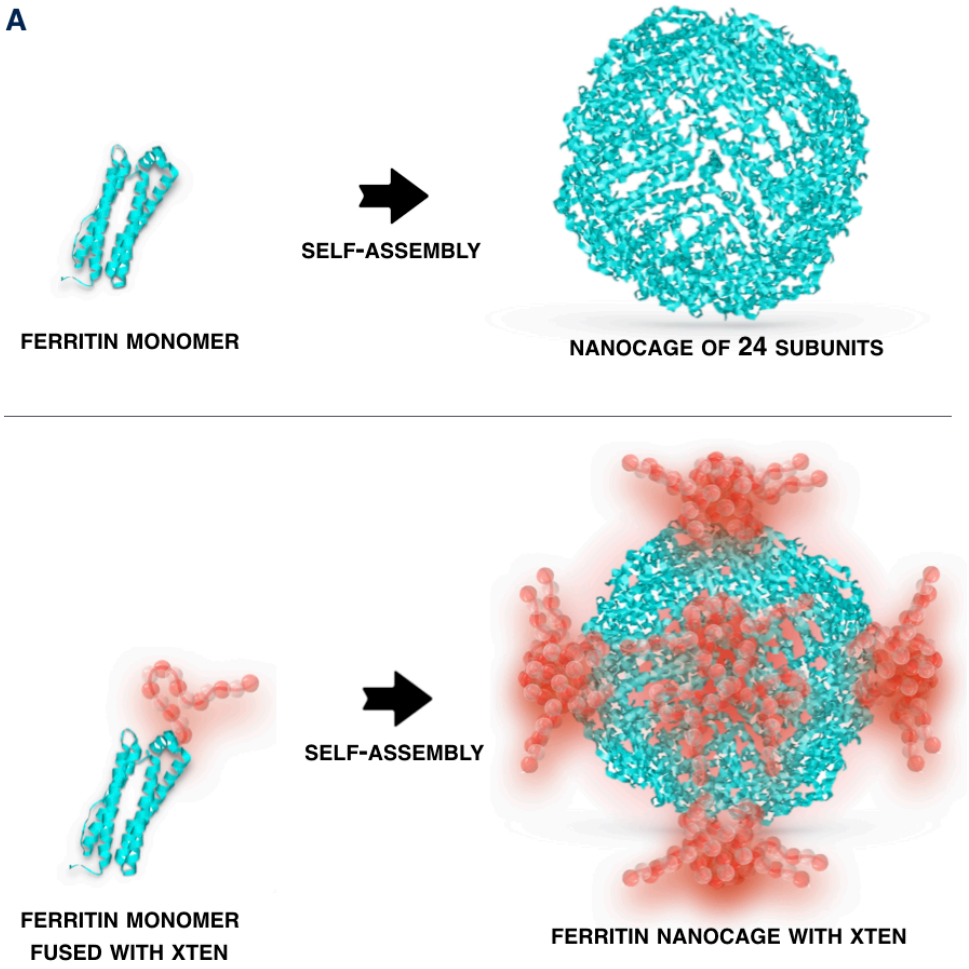

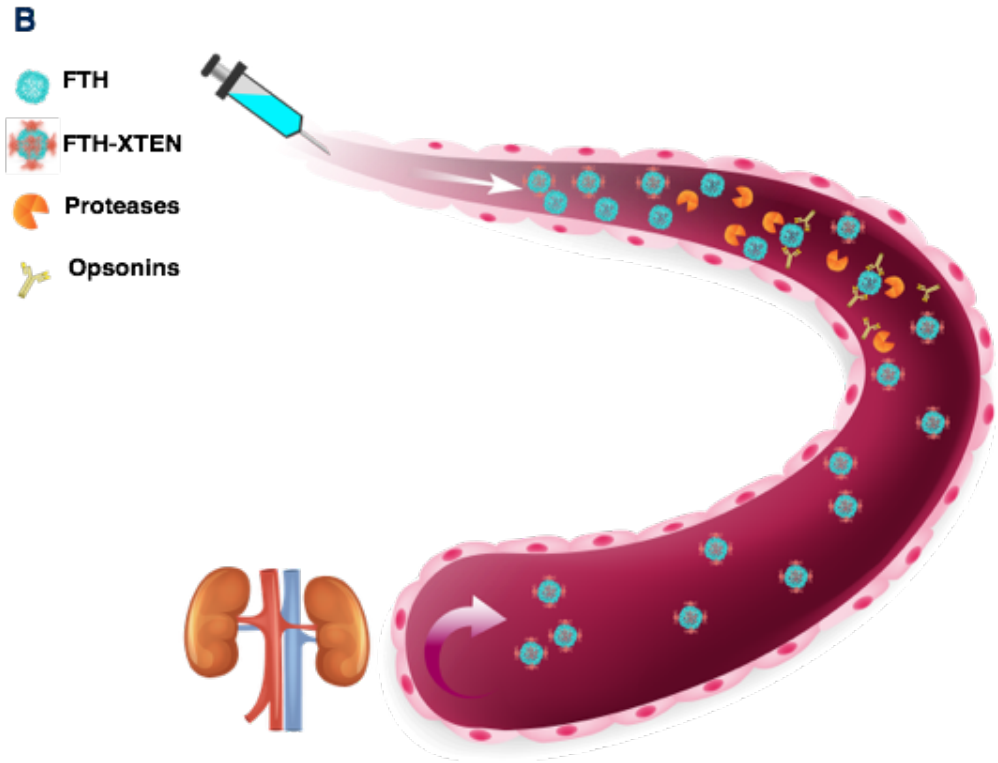

Figure 1. (A) Schematic diagram of the protein nanocage. (B) *In vivo* schematic diagram of the protein nanocage.

1. Introduction

Protein nanocages have a wide range of applicability in research due to their favourable features, such as high biocompatibility, low toxicity profiles and capacity for genetic and chemical modification. Thus they have gained an increasing amount of attention in the field of research for use as drug delivery vehicles of therapeutic drugs and peptides. However, they are prone to rapid degradation *in vivo* and approaches such as PEGylation that can overcome this issue are continuously being pursued. Due to the heterogeneous nature of PEG itself, chemical conjugation of PEG leads to poor quality control of its products. However, fusion of XTEN, a peptide composed of hydrophilic amino acids, can be done in a one step recombinant protein synthesis with high yields using bacteria *E. coli*. In this study, we have developed XTEN-fused ferritin nanocages with an extended pharmacokinetic profile that can be used as a platform for application in research.

Ferritins are endogenous proteins that exist ubiquitously in nature with a key role in iron homeostasis by the storage of excess iron in their core [1,2]. Ferritin's natural ability to absorb and store approximately 4500 iron (Fe^{3+}) irons is due to the presence of ion channels on its surface, and this feature can be used to load other metal ions in its core [1,3,4]. They are composed of heavy and light chains, where 24 monomers self-assemble into a multimeric spherical structure with inner and outer diameters of 8 and 12 nm, respectively [2,3]. Ferritins also comprise structural stability against non-native conditions, high pH (up to 9.0) and temperatures (up to 85°C), and high expression levels as a recombinant protein in efficient heterologous systems like *Escherichia coli* cells allow ferritin protein to be produced on a large-

scale, at high yield and at low cost, which is useful for industrial scale up purposes. Moreover, human ferritin shows high biocompatibility and stability in aqueous conditions, as well as low toxicity – which are all desirable features for applications in vivo [5,6].

Several researches have reported ferritin as a novel platform for application for delivery of either therapeutic drugs or peptides [4,6,7], as well as metal-based drugs in their internal cavity [4,5]. Ferritin protein possess external and internal interfaces with various chemical groups e.g. primary amines, thiols, which is available for genetic and chemical functionalization for targeted delivery of therapeutic or imaging agents [7,8]. Overall to summarize, ferritin has appropriate structural features, stability and applicability in modifications that endows it a novel platform as carriers in drug delivery.

In spite of these promising features, ferritin nanocages suffer from the limitations of all protein-based therapeutics - a short half-life. Further, although the enhanced permeability and retention (EPR) effect is fully exploited by the nanocages due to their adequate size, high levels of accumulation in the liver and fast clearance by the kidneys significantly decreases the residence time of the nanocages in circulation [9,10]. Ferritins undergo fast clearance from plasma, which has been observed in animal models after intravenous injection [11], and the presence of ferritin receptors on several cell types including macrophages [10,12] mediates rapid removal of ferritin from the circulation.

Thus for the purpose of extending the circulation half-life of the ferritin nanocages, a previously developed XTEN peptide [13,14,15,16] was conjugated as a 'protein cloud'. XTEN peptide is composed solely of hydrophilic amino acids (A, G, E, P, S, T) which when arranged, gathers a large hydrodynamic volume in a similar effect to PEGylation [13,17]. The peptide was genetically fused to ferritin monomers that self-assembles into the cage structure with the peptides displayed on the surface to form an outer layer. This hydrophilic protein cloud would: - provide a stealth effect to the nanocages against opsonization, protect against adsorption of serum proteins, reduce the rate of elimination by the kidneys and overall the modified ferritin nanocages would have a lengthened half-life.

Our experimental data supports that this strategy applied to develop long circulating ferritin nanocages provides an excellent nanocage platform for the delivery of drugs and therapeutic peptides.

2. Materials and methods

2.1 Biosynthesis of protein nanocages

The human ferritin heavy chain cDNA clone was purchased from Sino Biological Inc. (HG13217-G, China) in a pGEM-T Easy vector plasmid and recombinant XTEN gene synthesized by Cosmogenetech (Seoul, Korea).

Polymerase chain reaction (PCR) amplification was performed with these genes, using the appropriate primers (Table 1). Followed by an initialization step of 5 minutes at 95 °C, the denaturation, annealing and elongation steps were carried out at 95 °C, 54 °C and 72 °C for 30 seconds each for 25 cycles and an additional elongation step of 72 °C for 10 minutes followed. The amplified DNA mixed with a DNA loading dye (Takara A9501A) was analyzed for their size by gel electrophoresis using 1% agarose gel (SigmaAldrich A9539) premixed with nucleic acid gel stain Gelstar (Lonza 50535). After confirmation of DNA band size, the amplified DNA in agarose gel was cut and purified using a gel purification kit (Bioneer K-3035). PCR material was ligated into pGEM-T easy vector plasmids(amp^+) (Promega A1360) at 25 °C for one hour.

The ligated mixtures were transformed into Dh5alpha competent cells. All sterile conditions were maintained for experiments using *E. coli* competent cells. For plasmid DNA transformation, the competent cell aliquots stored in -80°C were thawed on ice, and total ligated mixture added to 100 ul of competent cells and heat shock was given at 42°C for 1 minute, followed by 2 minutes on ice and 200 ul of plain LB broth (Merck 1.10285) without antibiotics was added for stabilization at

37°C with shaking for 1 hour. The competent cell mixture was spread onto an LB agar plate ($amp^+X\text{-}gal^+IPTG^+$) and incubated overnight at 37 °C for blue-white screening and selection of plasmids with inserted gene. A single white colony was picked and resuspended in LB media, grown overnight and cells harvested for plasmid DNA purification using a purification kit (Intron biotechnology 17097).

In total, six gene clones were prepared: i) N-*NdeI*-H_6(hFTH)-*HindIII*-C; ii) N-*NdeI*-H_6(hFTH)-*XhoI*-linker-*BamHI*-(XTEN36)-*HindIII*-C; iii) N-*NdeI*-H_6(hFTH)- *XhoI*-linker-*BamHI*-(XTEN72)-*HindIII*-C; iv) N-*NdeI*-H_6(hFTH)-linker-*BamHI*-(XTEN144)-*HindIII*-C; v) N-*NdeI*-H_6(hFTH)-linker-*BamHI*-(XTEN288)-*HindIII*-C. The above gene clones were ligated into pT7-7 plasmids to construct the following expression vectors (Figure 2): pT7-wtFTH, pT7-FTH-X36, pT7-FTH-X72, pT7-FTH-X144, pT7-FTH-X288 encoding the synthesis of recombinant ferritin heavy chain then the glycine-rich linker-added XTEN peptide sequences of lengths 36, 72, 144, 288 amino acids, respectively. Final gene sequences in Pt7-7 plasmids were confirmed by sequencing by reading with a T7 primer (Cosmogenetech). The following descriptions of experimental methods applies to each of these recombinant proteins.

After complete sequencing, BL21 (gold DE3) *E. Coli* strain was transformed to express the above expression vectors in Pt7-7 plasmids(amp^+), and transformants with ampicillin resistance were selected. All growing conditions were at 37°C with aeration, using 2xYT media (16 gL^{-1} Bacto Tryptone BD211705, 10 gL^{-1} Yeast Extract BD212750, 5 gL^{-1} NaCl SigmaAldrich S5886) with the appropriate

ampicilin concentration. A single colony was selected and grown overnight for a primary culture that was used for scale-up to larger cultures the next day. Growing OD_{600} was allowed to reach 0.7 until 1 mM of isopropryl β-D-1-thiogalactopyranoside (IPTG) (Bioneer C-8001-2) was added for induction of recombinant gene transcription. The culture was then allowed to grow in the same conditions until final OD was over 3.0 and cell pellet collected by centrifugation of the culture at 6000 rpm.

For cell sonication, the pellet was resuspended in *E. Coli* lysis buffer, pH 8.0 (50 mM NaH_2PO_4 SigmaAldrich S8282, 300 mM NaCl, 10 mM Imidazole SigmaAldrich I2399) at a fifth of the original culture volume and protease inhibitor cocktail (Millipore 535140) was added at 1000x concentration. The lysis mixture was sonicated until appropriate clarity using the sonicator (Branson Digital Sonifier 120C) at amplitude setting 15% and the soluble portion was separated by centrifugation at 13,000 rpm at 4°C for.

This soluble portion was loaded onto a column and 5 ml lysate to 1 ml of Ni-NTA Agarose resin (Qiagen 30230) mixture was set for binding for 30 minutes at room temperature for wild type ferritin, and 2-hour binding at 4°C for XTEN fused proteins. After binding, the flow through was discarded and the columns washed by 20 ml of washing buffers, pH 8.0 (50 mM NaH_2PO_4, 300 mM NaCl, and 30 mM Imidazole for wild type ferritin and the same except for 50 mM Imidazole for XTEN fused proteins). Each column was then eluted with 3 ml of elution buffer, pH 8.0 (50 mM NaH_2PO_4, 300 mM NaCl, and 250 mM Imidazole) and the eluted

recombinant proteins collected in clean EP tubes. The eluted portions were gathered together and concentrated in a vivaspin 6 tube (Sartorius VS0602) through centrifugation at 4750 rpm and buffer was changed to dPBS at least four times. All centrifugation for wild type ferritin protein was at room temperature and 4°C for the modified proteins. As a final step, the proteins were centrifuged at 13,000 rpm for 10 minutes to remove for any aggregates and transferred into a new EP tube.

2.2 Characterization of protein nanocages

After recombinant wild-type and modified ferritin synthesis in *E. coli*, firstly the yield and purity was analyzed followed by confirmation of protein nanocage (PNC) structure formation. The PNCs were denatured by heating with SDS-PAGE loading buffer with mercaptoethanol for 10 minutes at 95°C and electrophoresis was carried out in reducing conditions on 10% polyacrylamide precast gels (Biorad 456-1036). The resulting gels were stained in a staining solution (Atto AE-1340) by microwaving for 30 seconds followed by shaking at room temperature for 20 minutes, and de-stained in distilled water by microwaving for 5 minutes. Stained gels were imaged using an imaging machine (AlphaImager HP).

Synthesized PNCs were then analyzed by fast protein liquid chromatography (FPLC) (Atka purifier 100) with a superdex column (Superdex 200 17-5175-01) with dPBS buffer. For sample preparation, PNC in dPBS was centrifuged at 13,000 rpm for 10 minutes to remove for any aggregates, filtered by centrifugation (Corning 05615000). In between every sample the column was washed with dPBS at least twice. With the total column volume of 24 ml, the eluent length was 1.5 and flow rate 0.4 $mlmin^{-1}$. Samples were injected into a 500 ul sample loop that gave a single high peak for absorbance at 280 nm (mAU).

Further, PNC size was analyzed by dynamic light scattering (DLS) by Zeta (Malvern, Zetasizer). Water was used as the dispersant and PNC samples of 1 $mgml^{-1}$ were prepared as the samples for FPLC were loaded into a cuvette

(Zetasizer) for measurement. Three measurements were taken for each PNC and the standard deviations stated.

Lastly, the synthesized PNCS were analysed by Tecnai transmission electron microscopy (Tecnai TEM). PNC samples of 1 $mgml^{-1}$ were prepared in the same way as above and further diluted with filtered dPBS to 0.025 $mgml^{-1}$ for sample preparation. Copper grids (Ted pella 01801) were plasma treated before sample loading and every removal of solutions were done using filter paper. PNC samples 7 ul were loaded onto the grids for 3 minutes, removed, followed by washing with 7 ul filtered water which was also removed. Uranium acetate solution was centrifuged briefly prior to use and 7 ul of the supernatant used for staining the grid for 30 seconds and also removed. Now ready copper grids were dried overnight in an unenclosed space before imaging.

2.3 *In vivo* pharmacokinetics by western blot

All experiments with live animals were performed in compliance with the relevant laws and institutional guidelines of Korea Institute of Science and Technology (KIST) and institutional committees have approved the experiments. Protein nanocages (3 mg/ml) in dPBS (100 ul) were intravenously injected via a tail vein into athymic nude mice of age 7 weeks (20 g, Orient, Seoul, Korea).

Chosen time points for detection were 5 minutes, 1, 2, 3, 6, 12, 24, 36, 48, 72 hours. At given time points post-injection, mice were anaesthetized, and blood was collected by the intraorbital space from mice in EP tubes prepared with 50 ul of 3.8% citric acid solution, pH 7.4 and placed on ice until centrifugation at 13,000 rpm for 10 minutes at 4°C to collect the serum. Separated serum was diluted with dPBS and SDS-PAGE loading dye, boiled at 95°C for 9 minutes and aliquoted for repeated analysis at -80°C.

Serum samples were further diluted threefold for analysis (a total dilution factor 6 from original serum) by Western blot with dPBS and SDS-PAGE loading dye in total volume. 10% Polyacrylamide gels were used with an SDS-PAGE marker (Biomax 1000) and electrophoresis performed for 1 hour at 160 V. The gel was transferred onto a nitrocellulose membrane in a semi-wet transfer machine (Biorad Trans-Blot Turbo) using material from a transfer kit (Biorad 170-4270) and all buffers used throughout the experiments from hereon was TBS (Biosesang T2005) with 0.1% Tween 20 (SigmaAldrich P7949). After transfer, the membrane was blocked for 1 hour at room temperature with shaking in buffer with 5% skim milk

and anti-ferritin heavy chain polyclonal antibody (Abcam ab65080) applied with 5% skim milk at 1:1000 ratio overnight at 4°C with gentle shaking. Followed by 2 hour washing with buffer, anti-rabbit IgG secondary antibody (SigmaAldrich A0545) with 5% skim milk was applied at 1:4000 with gentle shaking for 1 hour and then washed for further 2 hours. The washed membranes were transferred to a clean container and 1 ml of a 1:1 mixture of Clarity Western ECL substrate (Biorad) was applied to the membrane and pipetted thoroughly to ensure even distribution of the substrate. The membrane was placed between clean OHP films and western blot images were obtained using (Biorad Chemidoc).

2.4 Preparation of cy5-labelled protein nanocages

The purified PNCs in 0.1 M sodium bicarbonate solution (pH 8.4) were incubated with 1:24 PNC to dye molar ratio of Cy5-NHS Ester (Lumiprobe 43020) (excitation and emission maximum of 620 and 665 nm, respectively). Conjugation volume ratio was 10 ul dye in DMSO added to total volume 1 ml of PNC in the bicarbonate buffer. After 1 h at 25°C with shaking, the incubation mixture was loaded onto PD-10 columns (GE 52-1308) pre-equilibrated with dPBS and the conjugated PNC subsequently eluted with dPBS to leave behind the free dye in the column. The eluted protein was concentrated using an amicon centrifugal (Amicon Ultra 10K, Millipore, TECAN, Austria UFC4010BK) and then aggregates removed at the end by centrifugation at 13,000 rpm at 4°C for 10 minutes. For PNC preparation for *in vivo* experiments, the PNC concentration was calculated by Bradford's assay using the kit (Biorad 500-0006). Equal concentrations of PNCs (mg/ml) were used for each pharmacokinetics experiment.

Due to varying fluorescence labelling efficiencies, a standard curve was drawn for each PNC, by mixing a concentrated Cy5-labelled PNC with fresh mice serum and diluting the samples for fluorescence measurement. A standard curve was drawn for each PNC, with a line of best fit each that had R^2 values higher than 0.99. Thus produced standard curve was used in order to quantify the fluorescence values detected into protein concentrations in $mgml^{-1}$. These measurements were all performed on a black 96-well microplate (ThermoScientific Nunc 37105) and read by a fluorescence detector (Perkin Elmer EnVision 2103) for detection for Cy5 at 620 and 665 nm.

2.5 *In vivo* pharmacokinetics by fluorescence measurement

All experiments with live animals were performed in compliance with the relevant laws and institutional guidelines of Korea Institute of Science and Technology (KIST) and institutional committees have approved the experiments. Protein nanoparticles (10 mg/ml) in dPBS (100 ul) were intravenously injected via a tail vein into athymic nude mice of age 7 weeks (20 g, Orient, Seoul, Korea).

Chosen time points for detection were 5, 15, 30, 45 minutes, then 1, 3, 6, 12, 24, 48, 72 hours. At given time points post-injection, mice were anaesthetized, blood was collected by the intraorbital space from mice in EP tubes prepared with 50 ul of 3.8% citric acid solution, pH 7.4 and placed on ice until centrifugation at 13,000 rpm for 10 minutes at 4°C to collect the serum. Separated serum was transferred into a fresh EP tube and then analyzed straightaway on a black 96-well microplate with 50ul measurement volumes. Fluorescence detection was performed at excitation and emission wavelengths 620 and 665 nm and at least three readings were performed for each sample, meaning each animal, to be averaged for analysis. Quenched fluorescence values for time points under 1 hour were detected by diluting the samples by tenfold with fresh serum from mice.

Quantified serum PNC concentrations ($mgml^{-1}$) calculated from the standard curves were analyzed by WinNonlin software using a compartment-independent model, and the pharmacokinetic parameters of the five different PNCs were compared.

3. Results

3.1 Expression and purification of protein nanocages

3.1.1 Protein nanocage design

The modified protein nanocages were designed for the purpose of ensuring best coverage of the nanocage surface; at the same time, the objective was to minimize the length of XTEN as 24 of such peptides would be displayed on its surface. Both the N- and C-terminal addition of XTEN was investigated experimentally, and despite the hydrophilic nature of the XTEN peptide, the solubility profile of FTH-XTEN was visibly higher than XTEN-FTH. Further, a glycine-rich linker was also added in the place prior to the XTEN gene to further protrude the peptide on the nanocage surface. This glycine-rich linker is also non-structural in its nature, thus it would become an extension to the 'protein cloud', that is XTEN an intrinsically disordered protein, on the outer surface of the PNC. Thus altogether the structural composition of the PNC were the following: - polyhistidine tag (H_6) for Ni^{2+} affinity purification; recombinant human ferritin heavy chain; glycine-rich linker; XTEN (Figure 2).

All PNC constructs were readily expressed and synthesised in *E. coli* with high yields, as seen as the recombinant protein bands in Figure 3. The most notable feature of XTEN peptide of its physicochemical properties was its extremely high hydrophilicity. With increasing length of XTEN attached, the PNC stability and solubility increased in changing buffer conditions, pH and temperatures.

wtFTH	**CATATGCATCACCATCACCATCACACGACC**
	CTCGAGGCTTTCATTATCACT
	GGATCCTTCATCCACACCCGCTTTCTGAGAGCC
XTEN	**AAGCTTGAGGGTGGTAGCGAAGGCTCTGAAGGTGAG**
	ATCGATTTAGCCTTCGCCAGAGCCTTCGGAACCTTCACC
FTH-X36	**AAGCTTGAGGGTGGTAGCGAAGGC**
	ATCGATTTAACCCTCACCAGAACC
FTH-X72	**GGATCCGAGGGTGGTAGCGAAGGCTCTGAAGGTGAG**
	AAGCTTTTAGCCTTCGCCAGAGCCTTCGGAACCTTC
FTH-X144	**GGATCCGGGGGCACCTCCACCCCT**
	AAGCTTTTAGCCAGGGGCTGTGGAACT
	AAGCTTTTAGCCAGGGGCTGTGGAACT
FTH-X288	**GGATCCGGGGGCACCTCCACCCCT**
	AAGCTTACCACCGCCCGGAGCAGT

Table 1. Primer list. Shows a complete list of primers used in the cloning of protein nanocages in this study.

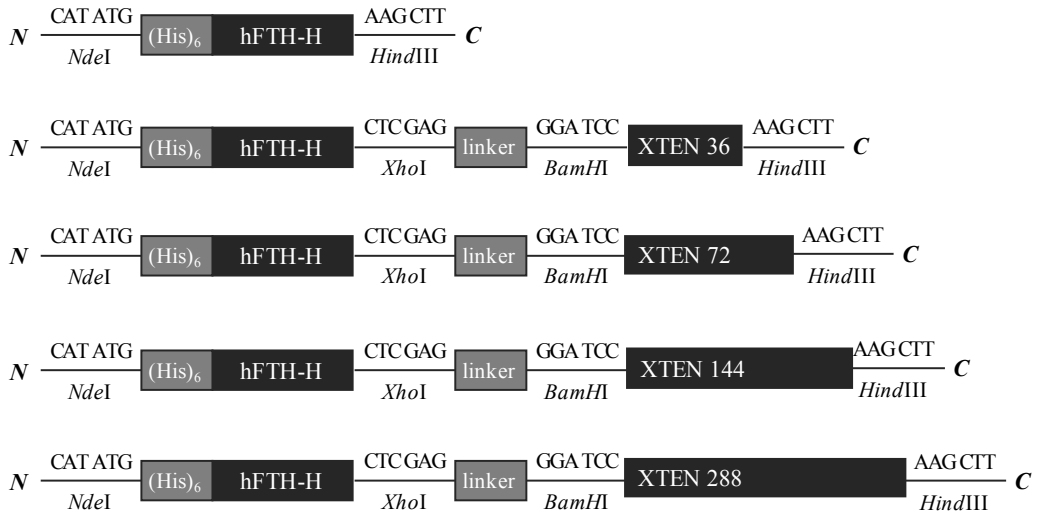

Figure 2. Vector map. Shows a complete list of recombinant genes inserted into the multiple cloning site in the production of the protein nanocages.

3.1.2 Protein nanocage purification

Analysis by SDS-PAGE (Figure 3) shows successful recombinant protein production for all protein nanocages. However, the width of the main band seems to decrease with increasing length of XTEN, in other words decreasing yield for protein synthesis with the same conditions. Further, analysis of solely the SDS-PAGE image may result in an underestimated level of purity for the recombinant protein produced. This is because previous reports with XTEN peptide show that degradation of the peptide occurs with the addition of beta-mercaptoethanol, in reducing conditions. Nevertheless, our result shows a thick band of recombinant protein produced at the expected molecular weight, with the added hydrodynamic volume of XTEN peptide.

The molecular weights of PNCs based on their amino acid composition, and then the observed molecular weights in Figure 3 are as follows: - i) wtFTH: 21.5 kDa; ii) FTH-X36: 28.6 and 30 kDa ; iii) FTH-X72: 31.7 and 36 kDa; iv) FTH-X144: 38.2 and 58 kDa; v) FTH-X288: 51.6 and 90 kDa. The percentage increase between calculated and observed value also increases in an exponential manner, as expected for XTEN, a hydrophilic globular protein.

Overall, based on the assumption that any bands shown below the main band of the recombinant protein are degraded forms of FTH-XTEN or XTEN by itself, further analysis of the synthesized proteins were proceeded as described in section 3.1.2.

3.2 Characterization of protein nanocages

3.2.1 FPLC

Synthesized PNCs were analyzed by FPLC to observe for successful nanocage formation, a multimeric protein, from the synthesized monomeric peptides. A sharp, high peak at the expected elution fraction confirmed that nanocage structure formation was successful for all five PNCs synthesized. The additional small peaks at a much later fraction, can be dismissed with the support of the following notions. Ferritin protein monomers do not exist by themselves but have an extremely high tendency to gather and form multimers. Due to the highly structurally stable nature of both ferritin and XTEN proteins, there is very little possibility of either two proteins being degraded to produce pieces of peptide debris during the short time period of sample preparation. Thus, although the samples were centrifuged and filtered prior to analysis, the peaks at the end can be dismissed as insignificant.

3.2.2 DLS

Dynamic light scattering results show singular peaks for all five PNCs synthesized. Modified PNC sizes increased from the wild type ferritin nanocage of 11 nm measured by DLS. The results were the following shown in Figure 3, where all four modified PNC sizes were measured to approximately 15 nm. Despite considering the standard deviation values, the four modified PNCs seem to be measured to approximately the same size.

3.2.3 TEM

Tecnai TEM equipment was used to observe the 12~15 nm size of FTH and FTH-XTEN nanocages as shown in Figure 3. The resolution of the TEM images, at the nanoscale do not allow for accurate estimations of the PNC size observed. However, intact cage-like morphology was confirmed for all five constructs synthesized. Thus ferritin monomers, with the addition of long XTEN peptides with large hydrodynamic volumes, successfully self-assemble to form the spherical cage protein with uniform PNC sizes.

WTFTH

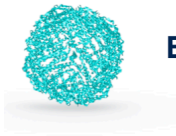

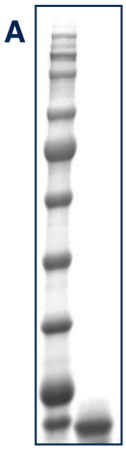

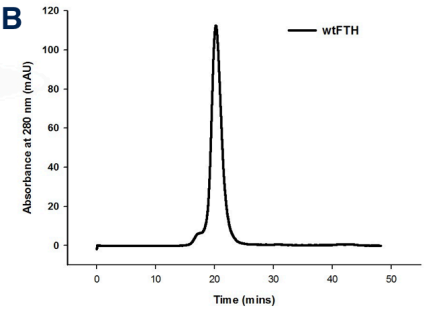

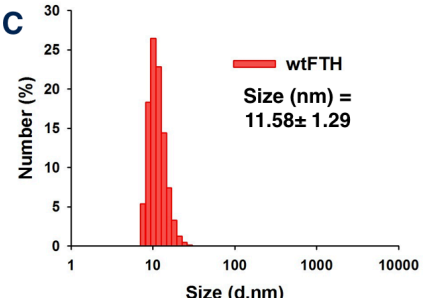

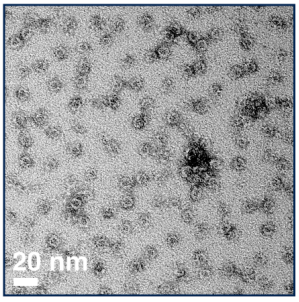

FTH-X36

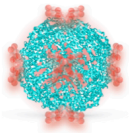

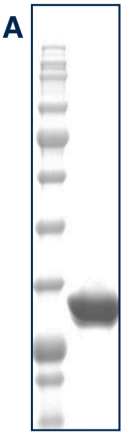

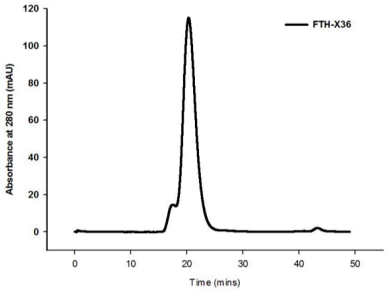

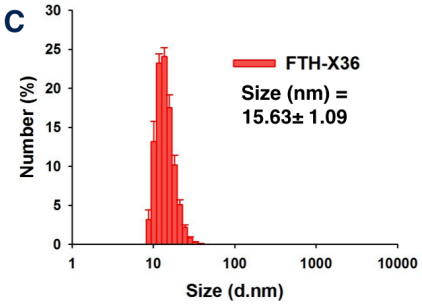

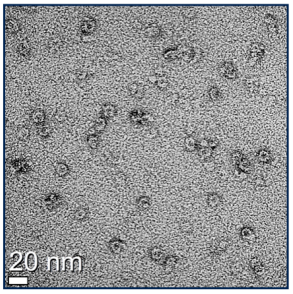

FTH-X72

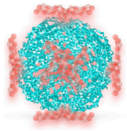

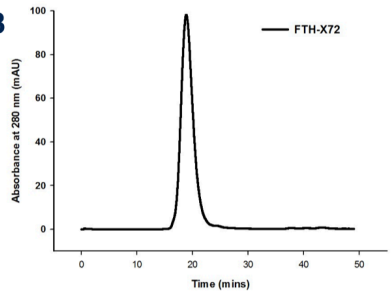

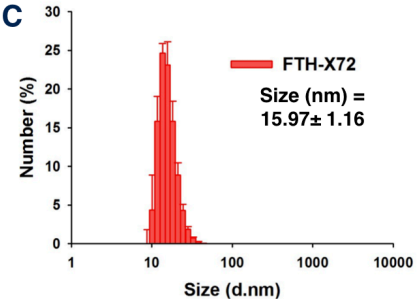

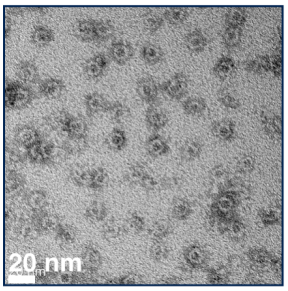

FTH-X144

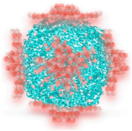

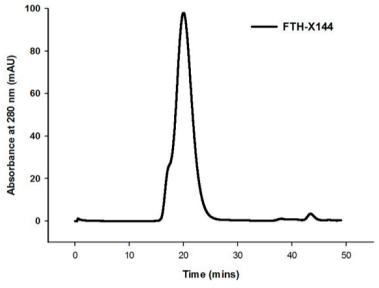

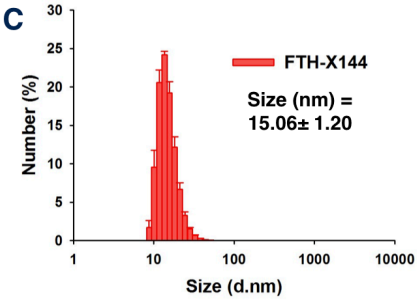

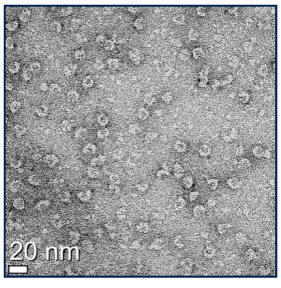

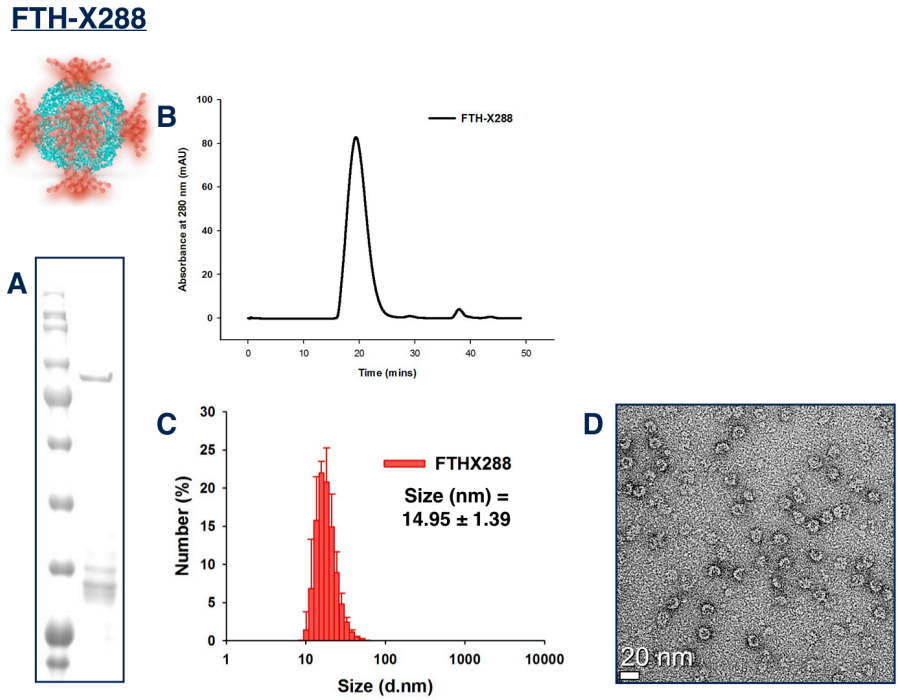

Figure 3. (A) SDS-PAGE analysis shows successful recombinant protein production for all protein nanocages (B) Fast liquid protein chromatography (FPLC) shows presence of multimers and absence of monomers, (C) Dynamic light scattering (DLS) for analysis of nanocage size, showing a single peak, (D) Tomography electron microscopy (TEM) shows intact morphology of all nanocages.

3.3 In vivo pharmacokinetics analysis

3.3.1 Western Blot analysis

In order to determine the residence time *in vivo* of wild type and modified ferritin nanocages, a pharmacokinetics study was carried out in mouse models. Based on the hypothesis that the XTEN protein cloud would slow the rate of degradation and elimination of the PNCs, appropriate time points were selected in order to determine the differences of pattern for the behaviour of the five PNCs *in vivo.* At the chosen time points after administration of the PNCs, blood was drawn from mice and serum separated to firstly investigate the presence/absence of the PNC. The result in Figure 4 shows clearly that the *in vivo* degradation of the PNC was markedly slowed as the final detection time for the PNC increases with increasing length of XTEN attached. Wild type ferritin can no longer be detected after 6 hours but the PNC with longest XTEN attached can be detected at 48 hours.

It is important to note that detection of this denatured form of ferritin, since the serum was boiled with mercaptoethanol, does not imply the presence of a full cage structure PNC. However, this pattern of data as seen in Figure 4 gives us a clear picture of the increased residence time and an approximate time-scale for further quantitative pharmacokinetic analysis (section 3.3.2).

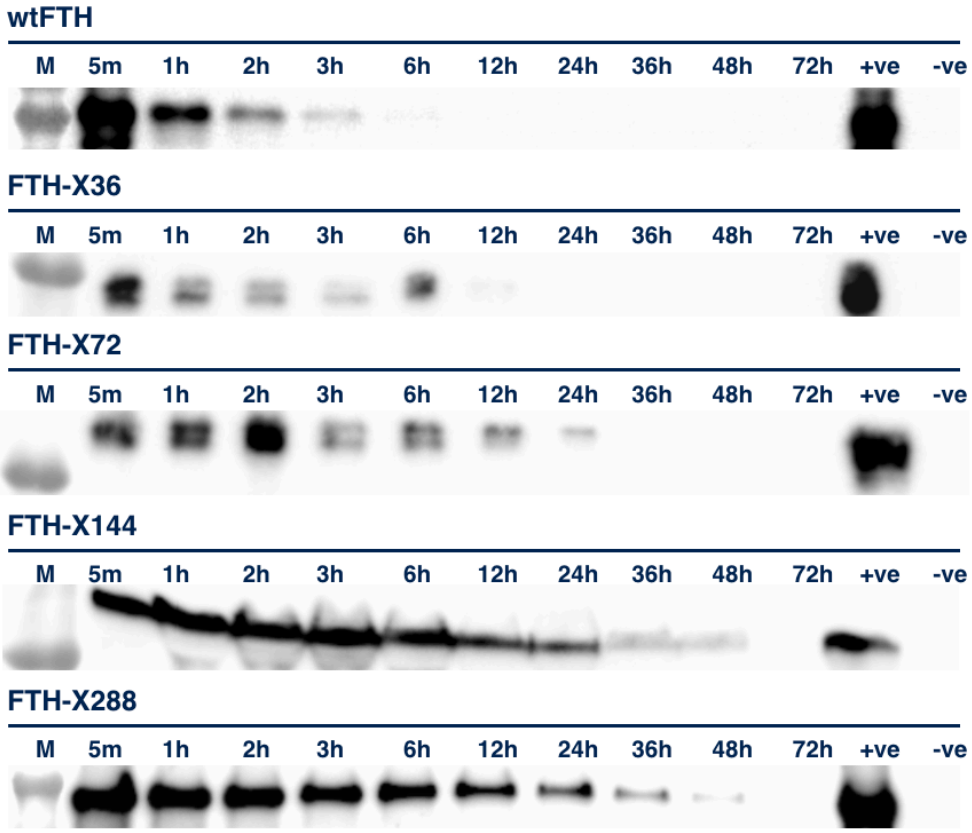

Figure 4. Western Blot analysis. Pharmacokinetics of FTH and FTH-XTEN nanocages were analyzed by Western blot, by detecting the presence of denatured FTH protein in serum samples taken at each time point. Results show increasing maximal detection point in correlation to increasing length of the XTEN peptide attached.

3.3.2 Fluorescence measurement

Followed by the pharmacokinetics analysis by Western blotting, a more quantitative approach was taken in order to obtain the pharmacokinetic parameters of the PNCs and modified PNCs.

PNCs were fluorescently labelled with Cy5-NHS Ester dye at 50 $mgkg^{-1}$ were administered into mice models and this dosage was determined following preliminary studies that revealed a high detection limit for the wild type and modified ferritin nanocages. The time points of this pharmacokinetics study was determined based on two factors, firstly the results of the western blotting experiment and secondly the appropriate time point data necessary for input into the WinNonlin software (a pharmacokinetics analysis and prediction program). Further, the fluorescence values for all PNCs under the 1 hour time post-injection were expected be above the saturated values for the machine's maximum fluorescence detection limit and thus they were measured at non- and tenth-diluted values. Thus at the chosen time points as mentioned in section 2.5, blood was drawn from mice and fluorescence values of the serum collected measured.

For analysis of the experimentally obtained values, a standard curve had to be drawn to quantify (in $mgml^{-1}$) the Cy-conjugated PNC from serum fluorescence values. Moreover due to the differences in the labelling of the Cy dye to the PNC, a standard curve had to be drawn for each PNC. The *in vivo* pharmacokinetics experiments ran parallel as individual set of experiments. All buffers, dosages,

concentrations, and experimental conditions in the preparation steps as well as the animal models of these experiments were equal.

The results of this pharmacokinetics analysis was done using compartment-independent modelling by the WinNonlin software. Results show lengthened half-life ($t_{1/2}$) and mean residence time (MRT), as well as reduced volume of distribution and clearance rates with the addition of XTEN (Table 2 and Figure 5). The half-life of wild type ferritin is calculated to 1 hour whereas nanocages with XTEN lengths 144 and 288 present values of 11.7 and 10.0 hours, respectively. Wild type ferritin nanocages showed rapid elimination *in vivo* with the clearance rate of 370 $mlhr^{-1}kg^{-1}$. On the other hand, modified nanocages show significantly decreased clearance rates as listed in Table 2, where the clearance rates drop to 72 then below 10 $mlhr^{-1}kg^{-1}$. Further, the calculated mean residence times in Table 2 are consistent with the Western Blot results shown in Figure 5.

This tenfold increase in half-life values for modified ferritin nanocage is a significant improvement to the 1 hour *in vivo* half life of the wild type ferritin nanocage.

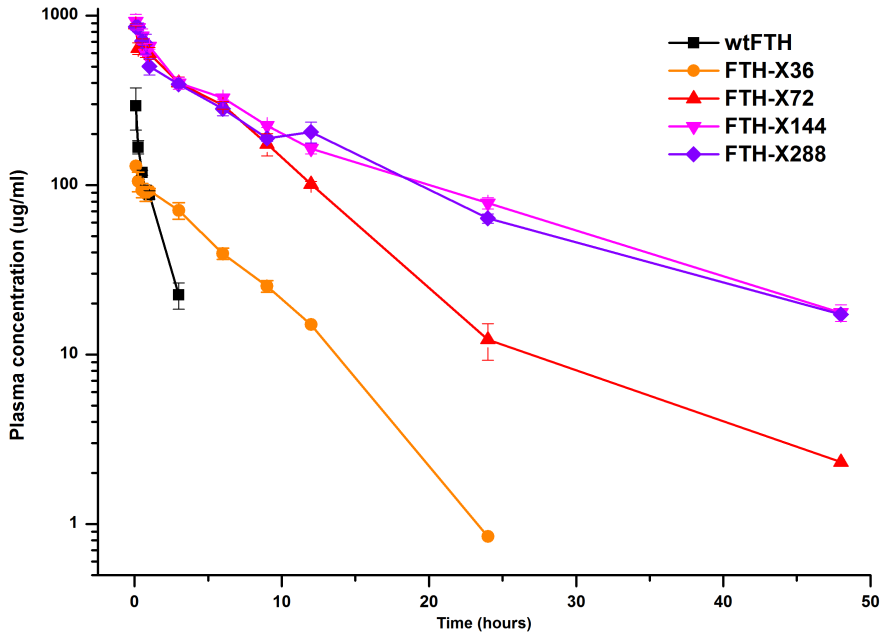

Figure 5. Plasma concentration graph shows the pharmacokinetic analysis of the protein nanocages after 50 $mgml^{-1}$ intravenous injection. Measured fluorescence intensities of serum samples collected at given time points after injection of FTH and FTH-XTEN nanocages labelled with Cy5-NHS Ester dye. Results show lengthened half-life, reduced volume of distribution as well as clearance with increasing length of XTEN peptide attached.

Parameter	Administration 50 $mg.kg^{-1}$ (i.v.)				
	wtFTH	FTH-X36	FTH-X72	FTH-X144	FTH-X288
$t_{1/2}$ (hr)	1.0	3.2	5.4	11.8	10.1
MRT (hr)	0.8	5.2	6.3	10.8	10.7
V_d ($ml.kg^{-1}$)	370.2	334.4	82.5	114.4	107.4
Cl ($ml.hr^{-1}.kg^{-1}$)	254.8	72.8	10.6	6.73	7.38

Table 2. Pharmacokinetic parameters of ferritin and modified ferritin nanocages are shown here.

4. Discussion

The data presented above show that FTH-XTEN is an effective modification method for extending the half-life of ferritin nanocages, as the attachment of the XTEN peptide lengthens their half-life by a tenfold (Table 2.).

Similar to polyethylene glycol (PEG), the hydrophilic nature of the XTEN peptides is chiefly responsible for the various mechanisms that result in this lengthened half-life. Upon entering the circulation, the nanocages encounter opsonins and serum proteins that adsorb onto the nanocage surface and subsequently trigger a cascade of protein adsorption [18,19]. However, the hydrophilic layer of XTEN significantly decreases surface adsorption of both opsonins and serum proteins, which results in decreased opsonisation [20,21]. Subsequently, premature clearance of the nanocages by the reticuloendothelial system (RES) is significantly reduced, which in turn would mean decreased initial rate of elimination from the circulation. However, the wild-type ferritin nanocages are 12 nm and measurement of the modified forms are approximately 14~15 nm in size. Nanocages, though modified with the addition of XTEN, are highly susceptible to phagocytosis and cannot completely avoid removal by the RES and would thus accumulate in the liver.

The half-life of wild type ferritin is calculated to 1 hr whereas nanocages with XTEN lengths 144 and 288 present values of 11.7 and 10.0, respectively. The mean residence times also increase with increasing length of XTEN peptide attached. Moreover, the pharmacokinetic parameters – both the reduced values of clearance and volume of distribution, with increasing lengths of XTEN attached, altogether

supports the hypothesis of a longer retention time of nanocages in blood circulation. Ferritin nanocages are readily applied in research as drug delivery vehicles and imaging agents, and this modified form can provide a longer-lasting effect for the purpose aforementioned.

It is more important to note the difference in elimination profiles by the kidney for the unmodified and modified nanocages. The kidney's glomerular endothelial cell pore size is known to be approximately 5 nm [9] and rapid clearance of the wild type ferritin nanocages suggest fast degradation of the protein cage that results in their elimination. Wild type ferritin nanocages showed rapid elimination *in vivo* with the clearance rate of 370 $mlhr^{-1}kg^{-1}$. On the other hand, modified nanocages show significantly decreased clearance rates as listed in Table 2, where the clearance rates drop to 72 then below 10 $mlhr^{-1}kg^{-1}$. The large hydrodynamic volume by the addition of 24 XTEN peptides onto nanocage surface would decrease the rate of nanocage degradation in circulation, which would consequently slow their rate of kidney filtration.

Looking at the pharmacokinetic parameters of the nanocages obtained in *in vivo* mouse models (Table 2), there is a similar pattern for both the increase in half-life and decrease in clearance rate for the two longest XTENs. FTH-X144 and FTH-X288 show similar values for the two parameters despite doubling of the length of the peptide. Further, data presented in Figure 5. shows the same pattern of western blot results for the two nanocages, as well as both their final detection time for the denatured ferritin in serum being the 48 hr time point. This can be postulated to be

due to similar extent of surface coverage of the nanocage by the peptides attached. Surface coverage of any drug or agent is the key factor in controlling the degree of protein and opsonin adsorption [10,11,18,19,21]. Thus, consistent with the hypothesis, it can be determined from the experimental results that sufficient surface coverage of the nanocage were achieved by XTEN lengths 144 and 288.

Although the details of nanocage degradation *in vivo* are not shown in this study, it has already been proven in numerous studies [13,14,15,16,17] that fusing XTEN results in these aforementioned effects *in vivo*. In summary the results of the study support the hypothesis that attachment of XTEN peptide result in a lengthened half-life of nanocages in the circulation.

5. Conclusions

The data presented above show that FTH-XTEN is an effective modification method for extending the half-life of ferritin nanocages, as the attachment of the XTEN peptide lengthens their half-life by a tenfold. The half-life of wild type ferritin is calculated to 1 hour whereas nanocages with XTEN lengths 144 and 288 present values of 11.7 and 10.0 hours, respectively. In particular, the pharmacokinetic parameters – both the reduced values of clearance and volume of distribution, with increasing lengths of XTEN attached, supports the hypothesis of a longer retention time of nanocages in blood circulation.

Ferritin nanocages are readily applied in research as drug delivery vehicles and imaging agents, and this modified form can provide a longer-lasting effect for the drug or peptide delivery. This would particularly apply in the case of ferritin nanocage where the target site of action would be in circulation and the target reachable during circulation. Extension of half-life for certain protein- and peptide-therapeutics, can enhance its efficacy and decrease the dose frequency of the very short-lived protein-based agents. Overcoming a significant barrier of the short-lived protein-based nanocage would broaden the scope of application for ferritin nanocages and allow the full potential of this exceptional protein nanocage to be exploited for application in theragnosis.

References

[1] Jutz, G., van Rijn, P., Santos Miranda, B. and Böker, A., 2015. Ferritin: a versatile building block for bionanotechnology. *Chemical Reviews*, *115*(4), pp.1653-1701.

[2] Theil, E.C., 2013. Ferritin: the protein nanocage and iron biomineral in health and in disease. *Inorganic chemistry*, *52*(21), pp.12223-12233.

[3] Fan, K., Gao, L. and Yan, X., 2013. Human ferritin for tumor detection and therapy. *Wiley Interdisciplinary Reviews: Nanomedicine and Nanobiotechnology*, *5*(4), pp.287-298.

[4] Liang, M., Fan, K., Zhou, M., Duan, D., Zheng, J., Yang, D., Feng, J. and Yan, X., 2014. H-ferritin–nanocaged doxorubicin nanoparticles specifically target and kill tumors with a single-dose injection. *Proceedings of the National Academy of Sciences*, *111*(41), pp.14900-14905.

[5] Li, L., Zhang, L. and Knez, M., 2016. Comparison of two endogenous delivery agents in cancer therapy: Exosomes and ferritin. *Pharmacological research*,*110*, pp.1-9.

[6] MaHam, A., Tang, Z., Wu, H., Wang, J. and Lin, Y., 2009. Protein-Based Nanomedicine Platforms for Drug Delivery. *Small*, *5*(15), pp.1706-1721.

[7] Heger, Z., Skalickova, S., Zitka, O., Adam, V. and Kizek, R., 2014. Apoferritin applications in nanomedicine. *Nanomedicine*, *9*(14), pp.2233-2245.

[8] Jeon, J.O., Kim, S., Choi, E., Shin, K., Cha, K., So, I.S., Kim, S.J., Jun, E., Kim, D., Ahn, H.J. and Lee, B.H., 2013. Designed nanocage displaying ligand-specific peptide bunches for high affinity and biological activity. *ACS nano*, *7*(9), pp.7462-7471.

[9] Barreto, J.A., O'Malley, W., Kubeil, M., Graham, B., Stephan, H. and Spiccia, L., 2011. Nanomaterials: applications in cancer imaging and therapy. *Advanced Materials*, *23*(12).

[10] Aggarwal, P., Hall, J.B., McLeland, C.B., Dobrovolskaia, M.A. and McNeil, S.E., 2009. Nanoparticle interaction with plasma proteins as it relates to particle biodistribution, biocompatibility and therapeutic efficacy. *Advanced drug delivery reviews*, *61*(6), pp.428-437.

[11] Vannucci, L., Falvo, E., Fornara, M., Di Micco, P., Benada, O., Krizan, J., Svoboda, J., Hulikova-Capkova, K., Morea, V., Boffi, A. and Ceci, P., 2012.

Selective targeting of melanoma by PEG-masked protein-based multifunctional nanoparticles. *Int j nanomedicine*, *7*, pp.1489-1509.
[12] Mirshafiee, V., Kim, R., Park, S., Mahmoudi, M. and Kraft, M.L., 2016. Impact of protein pre-coating on the protein corona composition and nanoparticle cellular uptake. *Biomaterials*, *75*, pp.295-304.
[13] Schellenberger, V., Wang, C.W., Geething, N.C., Spink, B.J., Campbell, A., To, W., Scholle, M.D., Yin, Y., Yao, Y., Bogin, O. and Cleland, J.L., 2009. A recombinant polypeptide extends the in vivo half-life of peptides and proteins in a tunable manner. *Nature biotechnology*, *27*(12), pp.1186-1190.
[14] Geething, N.C., To, W., Spink, B.J., Scholle, M.D., Wang, C.W., Yin, Y., Yao, Y., Schellenberger, V., Cleland, J.L., Stemmer, W.P. and Silverman, J., 2010. Gcg-XTEN: an improved glucagon capable of preventing hypoglycemia without increasing baseline blood glucose. *PloS one*, *5*(4), p.e10175.
[15] Haeckel, A., Appler, F., Figge, L., Kratz, H., Lukas, M., Michel, R., Schnorr, J., Zille, M., Hamm, B. and Schellenberger, E., 2014. XTEN-annexin A5: XTEN allows complete expression of long-circulating protein-based imaging probes as recombinant alternative to PEGylation. *Journal of Nuclear Medicine*, *55*(3), pp.508-514.
[16] Ding, S., Song, M., Sim, B.C., Gu, C., Podust, V.N., Wang, C.W., McLaughlin, B., Shah, T.P., Lax, R., Gast, R. and Sharan, R., 2014. Multivalent antiviral XTEN–peptide conjugates with long in vivo half-life and enhanced solubility.*Bioconjugate chemistry*, *25*(7), pp.1351-1359.
[17] Cleland, J.L., Geething, N.C., Moore, J.A., Rogers, B.C., Spink, B.J., Wang, C.W., Alters, S.E., Stemmer, W.P. and Schellenberger, V., 2012. A novel long-acting human growth hormone fusion protein (vrs-317): enhanced in vivo potency and half-life. *Journal of pharmaceutical sciences*, *101*(8), pp.2744-2754.
[18] Szleifer, I., 1997. Protein adsorption on surfaces with grafted polymers: a theoretical approach. *Biophysical Journal*, *72*(2 Pt 1), p.595.
[19] Amin, M.L., Joo, J.Y., Yi, D.K. and An, S.S.A., 2015. Surface modification and local orientations of surface molecules in nanotherapeutics. *Journal of Controlled Release*, *207*, pp.131-142.
[20] Florence, A.T., 2012. “Targeting” nanoparticles: the constraints of physical laws and physical barriers. *Journal of controlled release*, *164*(2), pp.115-124.

[21] Roy, R., Kumar, S., Tripathi, A., Das, M. and Dwivedi, P.D., 2014. Interactive threats of nanoparticles to the biological system. *Immunology letters*, *158*(1), pp.79-87.

Abstract (Kor)

최근 단백질 나노입자들은 그의 고유의 구조적 특성, 균일한 입도 분포, 생체적합성 (biocompatibility) 등의 특성으로 체외 및 체내 진단, 백신, 약물전달 등 여러 분야에서 활발히 응용 연구되고 있다. 그 중에서도 페리틴 (Ferritin)은 인체유래 단백질 구형 나노입자로 체내에서 철을 저장하는 역할을 하며, 높은 구조적 안정성과 유전자 조작을 통한 펩티드 표면 표출 및 구형 중심부의 약물 적하 등의 다양한 구조적 가능성을 가지고 있다. 하지만 기존의 고분자 약물전달체들에 비해 고유의 짧은 반감기라는 한계점을 가지고 있다.

본 학위 논문에서는 페리틴 나노입자의 짧은 반감기를 향상시키기 위하여 페리틴 나노입자 표면에 XTEN (extended half-life) 펩티드를 표출시킨 나노입자를 개발하였다. XTEN 펩티드는 친수성 아미노산으로만 이루어져 단백질 치료제에 유전자 합성 방법으로 자체 융합시킬 수 있으며, polyethyelene glycol (PEG)와 유사한 큰 유체 체적 (hydrodynamic volume)을 지니어 합성된 펩티드 및 단백질의 체내 안정성 및 반감기를 향상시킬 수 있는 효과를 가지고 있다.

페리틴 표면에 다양한 길이의 XTEN 펩티드를 융합시킨 후, 박테리아에서 단백질 코로나(corona)로 쌓여진 Ferritin-XTEN (FTH-XTEN) 융합 나노입자를 제조하였다. 합성된 융합 나노입자의 체외 및 체내 특성을 확인한 결과 나노입자의 반감기가 융합된 XTEN 펩티드의 길이에 따라 늘어나는 것을 확인하였으며, 기존 나노입자에 비해 향상된 혈중내 안정성 및 반감기를 소유하는 것을 확인하였다. 이러한 결과들은 페리틴 나노입자가 지닌 짧은 반감기라는 한계점을 극복하고, 체내에서 효과적으로 약물 전달체 및 치료목적 펩티드 전달체로 사용될 수 있는 (응용) 가능성을 뒷받침 한다.

주요어: 단백질 나노입자, 페리틴, XTEN